

See discussions, stats, and author profiles for this publication at: <https://www.researchgate.net/publication/354944916>

# Heat transfer analysis of jet impinging on a curved surface

Article in *Materials Today Proceedings* · September 2021

DOI: 10.1016/j.matpr.2021.09.230

CITATIONS

2

READS

128

4 authors, including:



**Chirag Manjunath**

BMS College of Engineering

3 PUBLICATIONS 8 CITATIONS

SEE PROFILE



**Azeem Pasha**

Bangalore University

10 PUBLICATIONS 69 CITATIONS

SEE PROFILE



**Hasansab Jamadar**

Brindavan College

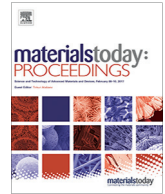
1 PUBLICATION 2 CITATIONS

SEE PROFILE



Contents lists available at ScienceDirect

## Materials Today: Proceedings

journal homepage: [www.elsevier.com/locate/matpr](http://www.elsevier.com/locate/matpr)

## Heat transfer analysis of jet impinging on a curved surface

Manjunath A.C.<sup>a</sup>, Azeem Pasha<sup>a</sup>, Hasansab Jamadar<sup>a</sup>, Manu Prasad M.P.<sup>b</sup><sup>a</sup> Department of Mechanical Engineering, Brindavan College of Engineering, Bangalore, Karnataka, India<sup>b</sup> Department of Mechanical Engineering, MVJ College of Engineering, Bangalore, Karnataka, India

## ARTICLE INFO

Article history:  
Available online xxx

Keywords:  
CFD  
Heat transfer enhancement  
Jet impingement  
k- $\epsilon$  Turbulence model  
V2f Turbulence model

## ABSTRACT

The detailed study on convection heat transfer and flow structure characteristic of air-jet studied with impinging vertically on a hemisphere plate. The inner surface of the cylindrical-shaped plate is subject to constant heat flux boundary conditions. Hemispherical plate subjected to comparative computations with Reynolds number (Re) ranging from 3000, 6000, and 9000 for the round nozzle impinging jet. Copyright © 2022 Elsevier Ltd. All rights reserved. Selection and peer-review under responsibility of the scientific committee of the International Conference on Smart and Sustainable Developments in Materials, Manufacturing and Energy Engineering

## 1. Introduction

Enhancement of heat transfer is an essential aspect in the industry; several techniques developed to improve.

Impinging jets use as cooling in industrial applications with localized heat transfer coefficients, representing a possible solution.

## 1.1. Impinged jet flow characteristics

When a fluid is forced out of a small opening called a jet. It is a submerged jet as it emerges through a small opening. Impinged jet flow pattern characterized with three regions, namely free, impinged & wall jet region. Free jet will not be influenced by impingement surface-characterization of impingement region seen with increased static pressure: with the decrease in mean axial velocity. Flow starts get accelerating as it approaches the impingement surface. At the end of the impingement surface, the pressure gradient becomes zero. The presence of the wall and stagnant fluid helps in developing differences in velocities at the wall region. The impingement layer helps in developing the boundary layer.

Quantifies heat transfer in a concave surface is 20% more than a flat surface. R.E [1]. The impinging circular jets on semi-circular surfaces, cooling surface, jet distance, and jet to jet spacing effectiveness [2]. Ring-shaped eddies form in the wall jet where the toroidal vortices reach the plate, which helps heat transfer [3]. The effect of impinging jet vertically on a smooth, hemispherical plate [4]. Nozzle shape and curvature effect on the concave surface with slot jet impingement [5]. Cooling of electronic components with

impinged submerged air-jet and nozzle-to-surface spacing [5]. Showed effect on different types of curvatures with increasing Reynolds number on the local Nusselt number [6].

## 2. Problem description

Fig. 1 shows Curved plate with physical domains. It consists of 2-dimensional jet of diameter "D" with a distance of "Z" above the impingement surface. Aluminium material is used for impingement surface with constant heat flux along curvature diameter "d". In a very small quantity loss occurs due to conduction and radiation.

## 2.1. Boundary conditions

Boundary condition plays a crucial role in CFD analysis. Physical model specified with boundary conditions of flow and thermal variables. All the boundary conditions specified are shown in Fig. 2

Inlet boundary: profile is considered as inlet boundary condition for different Reynolds number. The Reynolds number for inlet is assigned as Re = 3000, 6000 and 9000.

Outlet: outflow is used as outlet boundary condition as the pressure at the outlet is not clearly known.

Target wall: The target wall is defined as no-slip wall (i.e.  $u = 0$ ,  $v = 0$  m/s) with constant wall heat flux. In my computational domain aluminium impinging plate is used as a source of heat flux of 1000 W/m<sup>2</sup>. Also radiation is neglected.

Insulated wall: The upper insulated wall fluid boundary is set to adiabatic ( $Q = 0$  W/m<sup>2</sup>) no-slip wall ( $u = 0$ ,  $v = 0$  m/s) and conse-

<https://doi.org/10.1016/j.matpr.2021.09.230>

2214-7853/Copyright © 2022 Elsevier Ltd. All rights reserved.

Selection and peer-review under responsibility of the scientific committee of the International Conference on Smart and Sustainable Developments in Materials, Manufacturing and Energy Engineering

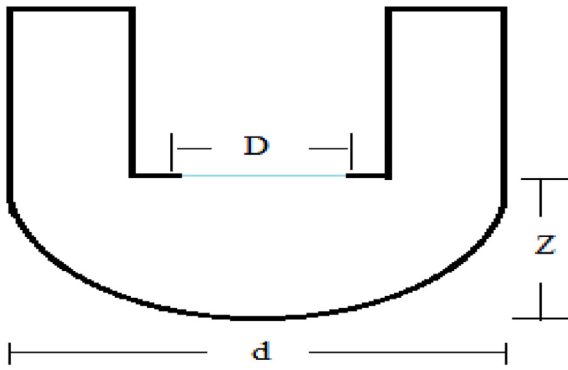


Fig. 1. Shows physical domain of curved plate.

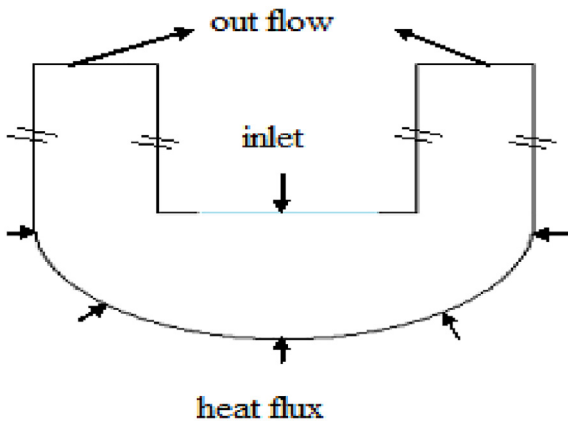


Fig. 2. Shows the physical domain of curved plate with boundary condition.

quently defines a confined jet. However, this is not believed to sensibly affect the results.

2.2. Meshing model of curved surface

2.3. Grid generation and approach

An impinging jet creates a complex flow-field and therefore, care must be taken in defining a computational grid that adequately captures the flow. Proper resolution to the region provided

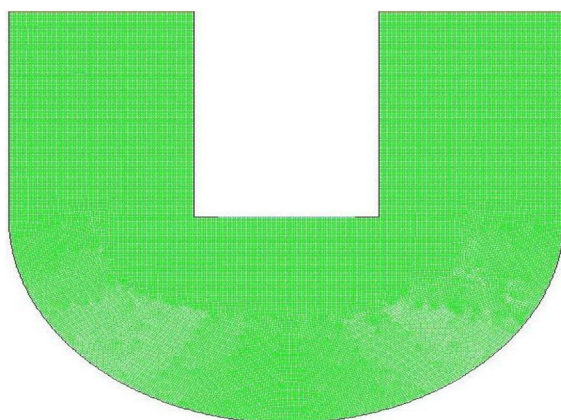


Fig. 3. Two Dimension Meshing Model of the curved plate.

to predict heat transfer and impingement fluid flow characteristics with grid-independence on the model.

The optimum grid system has the meshing resolution as shown in Fig. 3.

Grid cell was generated using Gambit, 42,157 elements of non uniform structure, a meshing program and CFD pre-processor.

2.4. Cases

All computational cases were solved using the k-ε and V2F turbulence model within FLUENT™ 6.3. The jet diameter was 0.003 m and the nozzle-plate spacing (Z/D) was 2, which fixed the computational domain length (L) at 0.033 m. Simulations were carried out with an impingement plate heat flux of 1000 W/m<sup>2</sup> and three different Reynolds numbers are 3,000, 6,000, and 9,000. The simulations were carried past the convergence point to ensure a stable solution had been achieved with the default relaxation values.

3. Results

The numerical analysis of the curved plate with air jet impingement on a using V2F model and the standard k-ε models were carried out. The results from fluids flow and heat transfer of an impinging air jet are presented and analysed in this chapter in the form of contours and graphs for three different Reynolds number (Re = 3000, 6000, 9000).

3.1. Contours of total temperature (Kelvin)

Contours of Total temperature for different Reynolds number are presented for standard k-ε model and v2f model are shown in Figs. 4-9. Form these contours, value of temperature for both the models are same in higher Reynolds number. If Reynolds number is higher the temperature will be decreases.

3.2. Contours of Turbulence intensity (%)

Contours of Turbulence Intensity for different Reynolds numbers are represented for standard k-ε Model and v2f model is shown in Figs. 10-15. and same thing observed in [7]. From the contours we can see that, value of Turbulence intensity is higher with increasing Reynolds number for both models. For Re = 9000, Turbulence intensity is higher in standard k-ε model than V2f model. Fig. 16.

3.2.1. Graphs

Fig. 6 shows Nusselt number variation along with radial distance. Below graph represents Radial distance and Nusselt number

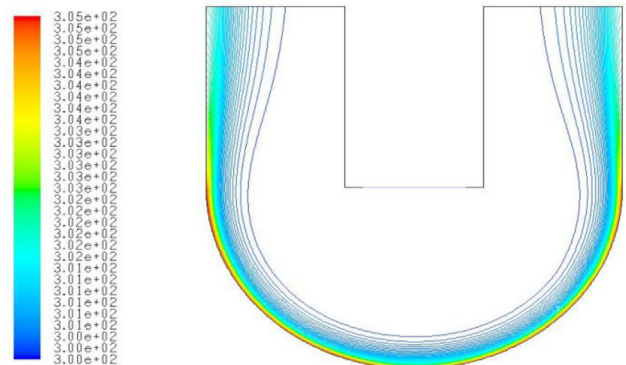


Fig. 4. Profiles of Total temperature for Re = 3000, k-ε Model.

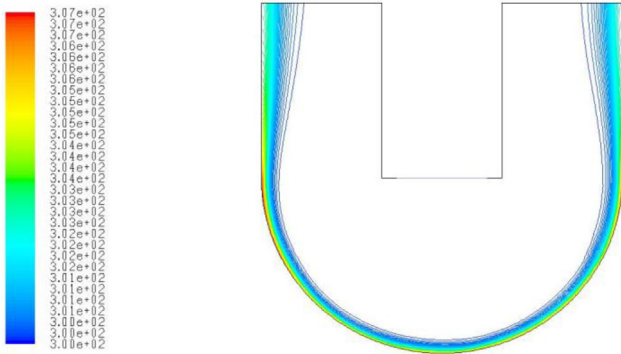


Fig. 5. Profiles of Total temperature for Re = 3000, V2F Model.

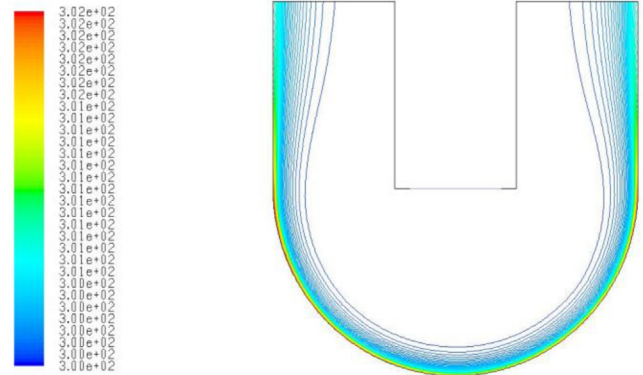


Fig. 8. Profiles of Total temperature for Re = 9000, k-ε Model.

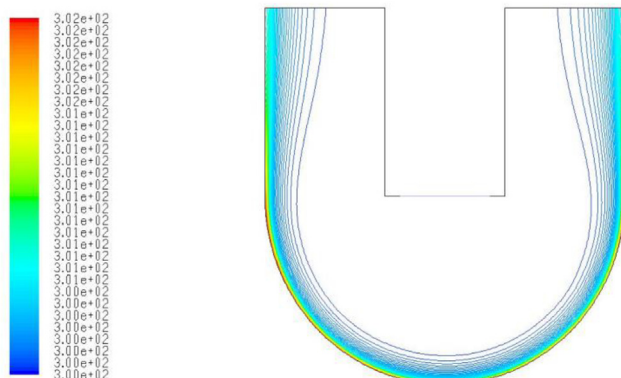


Fig. 6. Profiles of Total temperature for Re = 6000, k-ε Model.

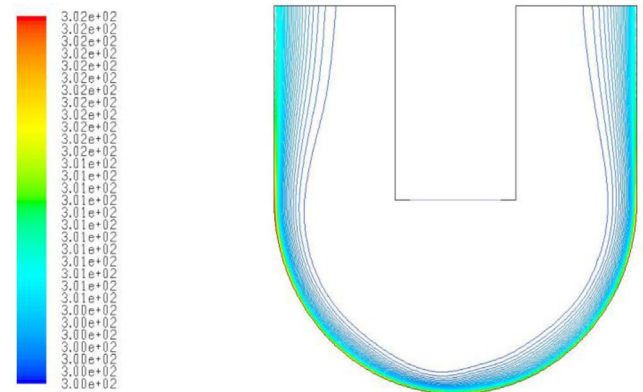


Fig. 9. Profiles of Total temperature for Re = 9000, V2F Model.

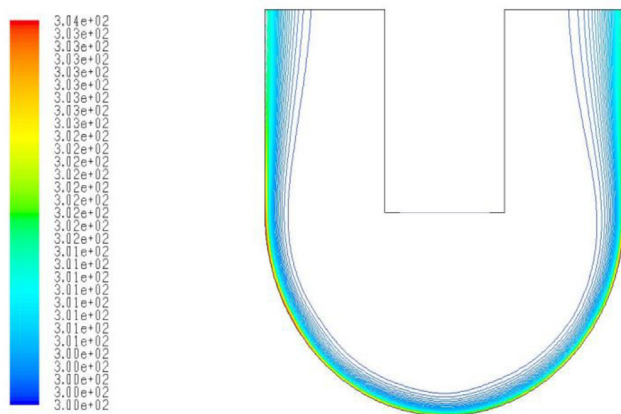


Fig. 7. Profiles of Total temperature for Re = 6000, V2F Model.

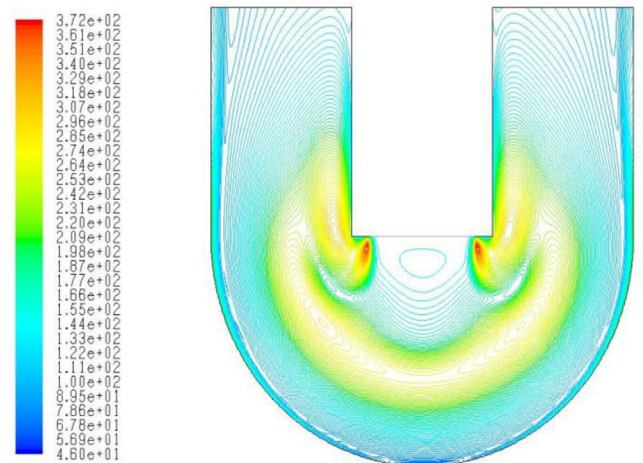


Fig. 10. Contours of Turbulence intensity for Re = 3000, standard k-ε Model.

along X & Y axis. Solid-fluid interface helps in controlling Nusselt number with temperature and heat flux. Time parameter increases these parameters. From the graph Nusselt number is higher in k-ε model than v2f model. Hence standard k-ε model gives the better result the v2f model.

Fig. 17 shows surface heat transfer variation along radial distance. From graphs surface heat increases with Reynolds number for both k-ε model and v2f model. Heat transfer coefficient is

higher in k-ε model than v2f model for all Reynolds number. Hence k-ε model is better than v2f model and similarity [8].

Variation of total pressure with different Reynolds number is shown in Fig. 18 the pressure is increasing with increasing Reynolds number. Total pressure is higher in standard k-ε model than V2f model.

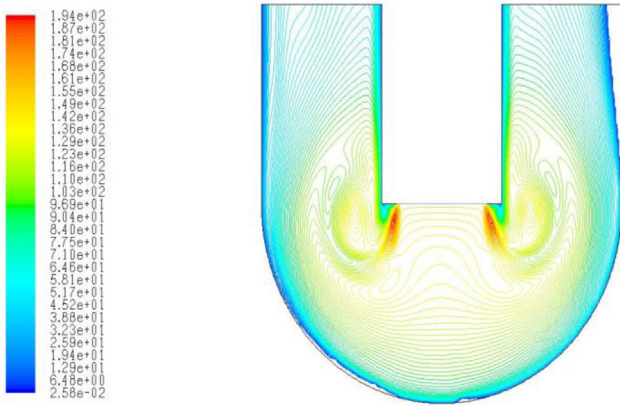


Fig. 11. Contours of Turbulence Intensity for Re = 3000, V2F Model.

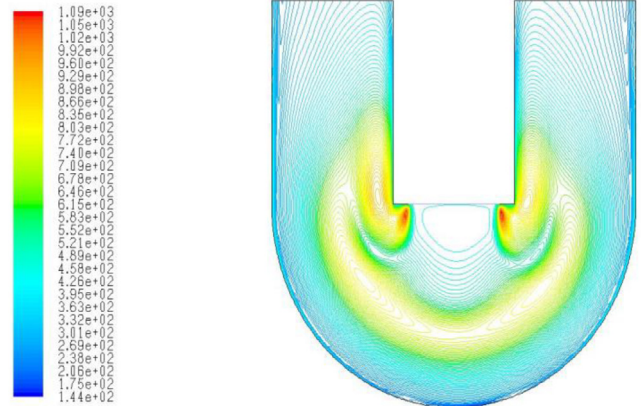


Fig. 14. Profiles of Turbulence intensity for Re = 9000, standard k-ε Model.

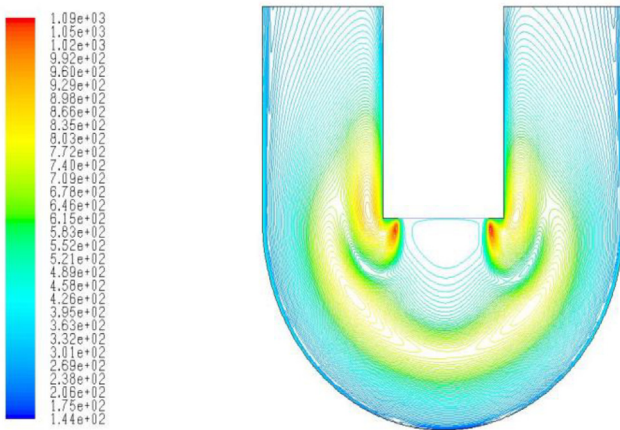


Fig. 12. Contours of Turbulence intensity for Re = 6000, standard k-ε Model.

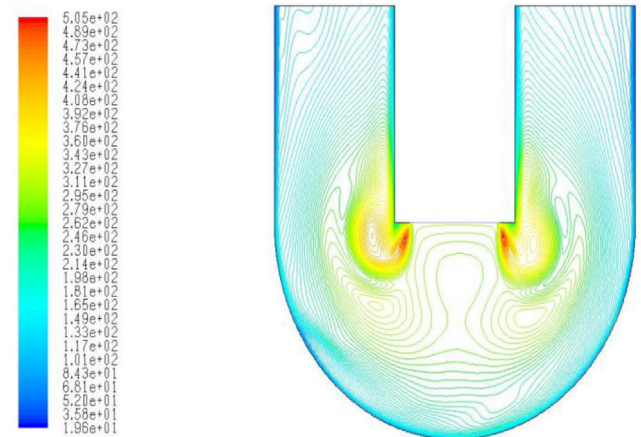


Fig. 15. Profiles of Turbulence Intensity for Re = 9000, V2F Model.

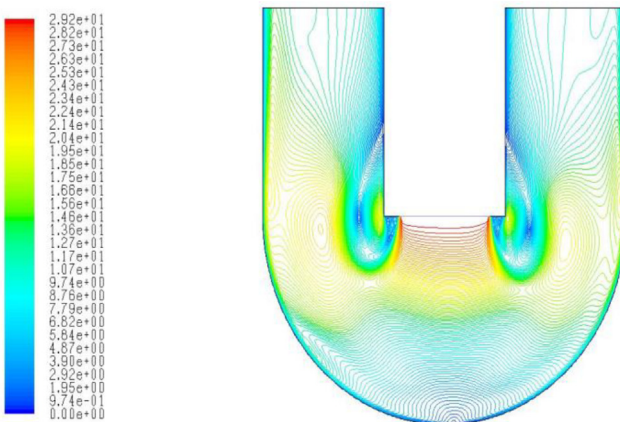


Fig. 13. Contours of Velocity Magnitude for Re = 6000, V2F Model.

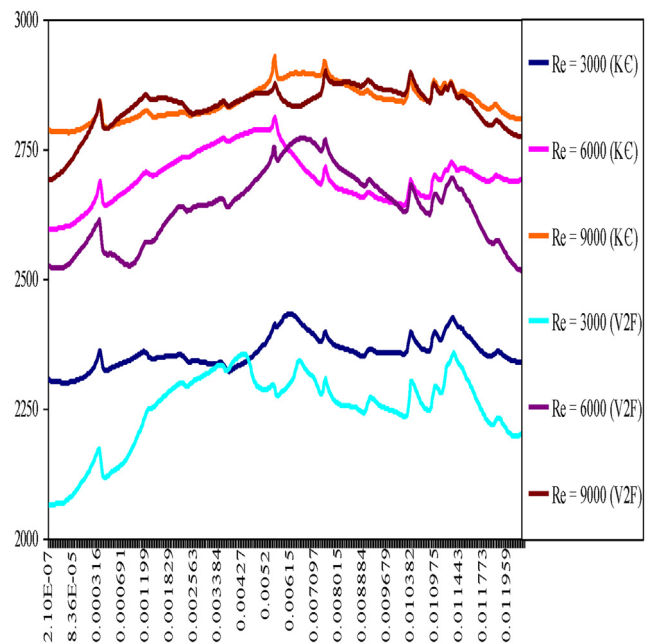


Fig. 16. Variation of Nusselt number with radial distance.

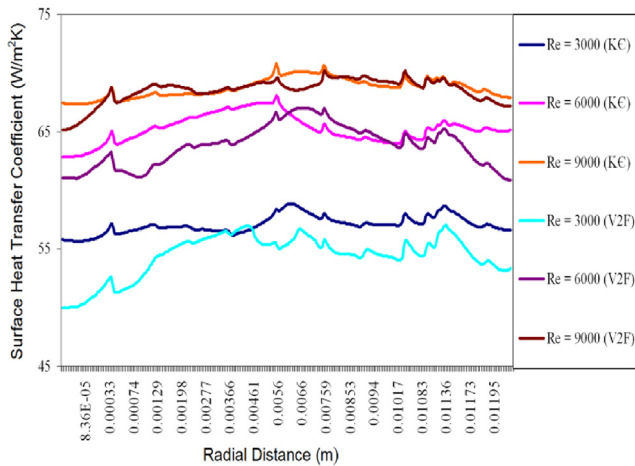


Fig. 17. Variation of surface heat transfer coefficient with radial distance.

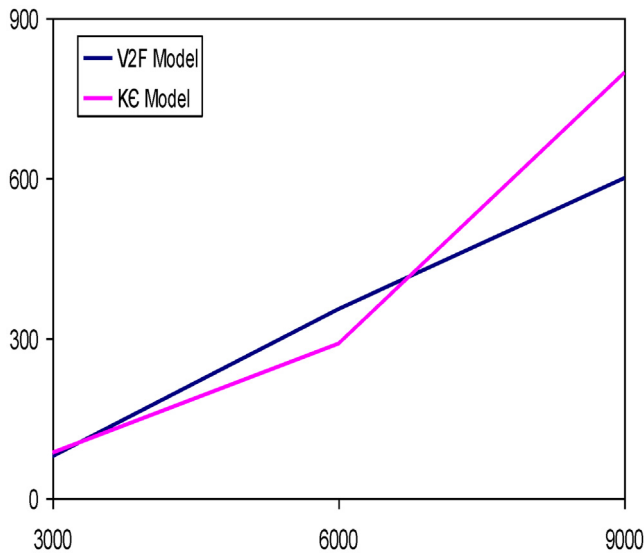


Fig. 18. Variation of total pressure with different Reynolds number.

#### 4. Conclusion

Heat transfer analysis during jet impingement on curved surfaces is carried out for different Reynolds number using V2F model

and the standard  $k-\epsilon$  models. From these analyses we are concluded that,

Total temperature for different Reynolds number is presented for standard  $k-\epsilon$  model and v2f model are shown in Figs. 4-9. Value of temperature for both the models are same in higher Reynolds number. If Reynolds number is higher the temperature will be decreases.

Turbulence Intensity for different Reynolds numbers are represented for standard  $k-\epsilon$  model and v2f model is shown in Figs. 10-15. From the contours we can see that, value of Turbulence intensity is higher with increasing Reynolds number for both models. For  $Re = 9000$ , Turbulence intensity is higher in  $k-\epsilon$  model than V2f model.

Surface heat transfer along with radial distance is shown in Fig. 17 and observed in [9]. It is predicted that heat transfer increases with Reynolds number for both standard  $k-\epsilon$  model and v2f model. From the above graph surface heat transfer coefficient is higher in  $k-\epsilon$  model than v2f model for all Reynolds number.

Hence from the results and graphs it is seen that the Standard  $k-\epsilon$  model is better than the V2F model for the cases considered.

#### CRediT authorship contribution statement

**Manjunath A.C.:** Visualization, Investigation. **Azeem Pasha:** Conceptualization, Writing – original draft, Writing – review & editing. **Hasansab Jamadar:** Supervision, Validation, Writing – review & editing, Validation. **Manu Prasad M.P.:** Methodology, Data curation.

#### Declaration of Competing Interest

The authors declare that they have no known competing financial interests or personal relationships that could have appeared to influence the work reported in this paper.

#### References

- [1] J.C. Rotta, *Phys. Fluids* 10 (1967) 283–292.
- [2] R.E. Chupp, H.E. Helms, P.W. McFadden, T.R. Brown, *J. Aircraft* 6 (1969) 203–208.
- [3] C.O. Popiel, O. Trass, *Exp. Therm Fluid Sci.* 4 (1991) 253–264.
- [4] S. Jachna, (1978).
- [5] G. Yang, M. Choi, J.S. Lee, *Int. J. Heat Mass Transf.* 42 (1999) 2199–2209.
- [6] C. Cornaro, A.S. Fleischer, M. Rounds, R.J. Goldstein, *Int. J. Therm. Sci.* 40 (2001) 890–898.
- [7] C. Yang, X. Zhang, X. Cao, J. Liu, F. He, *Procedia Eng.* 121 (2015) 1827–1835.
- [8] W.Z. Lu, C.M. Tam, A.Y.T. Leung, A.T. Howarth, *Num. Heat Trans. Part A: Appl.* 42 (2002) 233–251.
- [9] F. Iachachene, Y. Halouane, A. Mataoui, A. Benaissa, *Prog. Comput. Fluid Dyn.* 16 (2016) 179–189.